Cancer Immunology, Immunotherapy (2022) 71:1863–1875
https://doi.org/10.1007/s00262-021-03125-w

ORIGINAL ARTICLE

Functional virus-specific memory T cells survey glioblastoma

Jianfang Ning[1] · Noah V. Gavil[2] · Shaoping Wu[1] · Sathi Wijeyesinghe[2] · Eyob Weyu[2] · Jun Ma[1] · Ming Li[1] · Florina-Nicoleta Grigore[1] · Sanjay Dhawan[1] · Alexander G. J. Skorput[3] · Shawn C. Musial[3] · Clark C. Chen[1] · David Masopust[2] · Pamela C. Rosato[2,3]

Received: 28 September 2021 / Accepted: 24 November 2021 / Published online: 10 January 2022

Abstract

Glioblastoma multiforme (GBM) is among the most aggressive, treatment-resistant cancers, and despite standard of care surgery, radiation and chemotherapy, is invariably fatal. GBM is marked by local and systemic immunosuppression, contributing to resistance to existing immunotherapies that have had success in other tumor types. Memory T cells specific for previous infections reside in tissues throughout the host and are capable of rapid and potent immune activation. Here, we show that virus-specific memory CD8 + T cells expressing tissue-resident markers populate the mouse and human glioblastoma microenvironment. Reactivating virus-specific memory T cells through intratumoral delivery of adjuvant-free virus-derived peptide triggered local immune activation. This delivery translated to antineoplastic effects, which improved survival in a murine glioblastoma model. Our results indicate that virus-specific memory T cells are a significant part of the glioblastoma immune microenvironment and may be leveraged to promote anti-tumoral immunity.

Keywords Glioblastoma · Memory CD8 + T cell

Introduction

Glioblastoma multiforme (GBM) is a lethal form of malignant brain tumor and remains refractory to immunotherapies that have transformed the treatment of several cancers. With current standard of care, surgery followed by radiation, chemotherapy, and electric field therapy, median patient survival is less than 18 months. Glioblastoma intra-tumorigenicity and associated immunosuppression within the tumor microenvironment present unique challenges for therapeutic development [1, 2]. The presence of the blood–brain and blood–tumor barrier that restrict penetration of large macromolecules further limits antibody-based immunotherapies.

We recently described a novel form of immunotherapy that builds on the activation of virus-specific memory T cells abundant in tumors with no known viral etiology [3–8]. This therapy stems from the potent capacity of tissue-resident memory T cells (T_{RM}) to execute a 'sensing and alarm' function upon antigen re-exposure [9]. T_{RM} are a subset of memory T cells that reside within tissues, locally patrolling for reinfection and rarely reentering circulation [10, 11]. Once reactivated, T_{RM} produce pro-inflammatory cytokines that trigger local immune stimulation, and chemokines that recruit innate and adaptive immunity to the site of reactivation [9, 12, 13]. This T_{RM} sensing and alarm function can be triggered in mouse models of melanoma through delivery of viral-derived peptides alone. This form of immunotherapy is termed peptide alarm therapy (PAT) and leads to a significant reduction of tumor growth. When PAT is combined with PD-L1 checkpoint blockade, melanoma tumor burden can be entirely eliminated [3]. It remains unclear if this strategy can translate to tumors where the immunosuppressive environment dominates, such as GBM.

T cells with a T_{RM} phenotype have been identified in gliomas [14, 15], and we sought to assess the abundance

✉ Pamela C. Rosato
pamela.c.rosato@dartmouth.edu

1 Department of Neurosurgery, University of Minnesota, Minneapolis, MN 55455, USA

2 Center for Immunology, Department of Microbiology and Immunology, University of Minnesota, Minneapolis, MN 55455, USA

3 The Norris Cotton Cancer Center, Department of Microbiology and Immunology, Geisel School of Medicine at Dartmouth College, Lebanon, NH 03756, USA

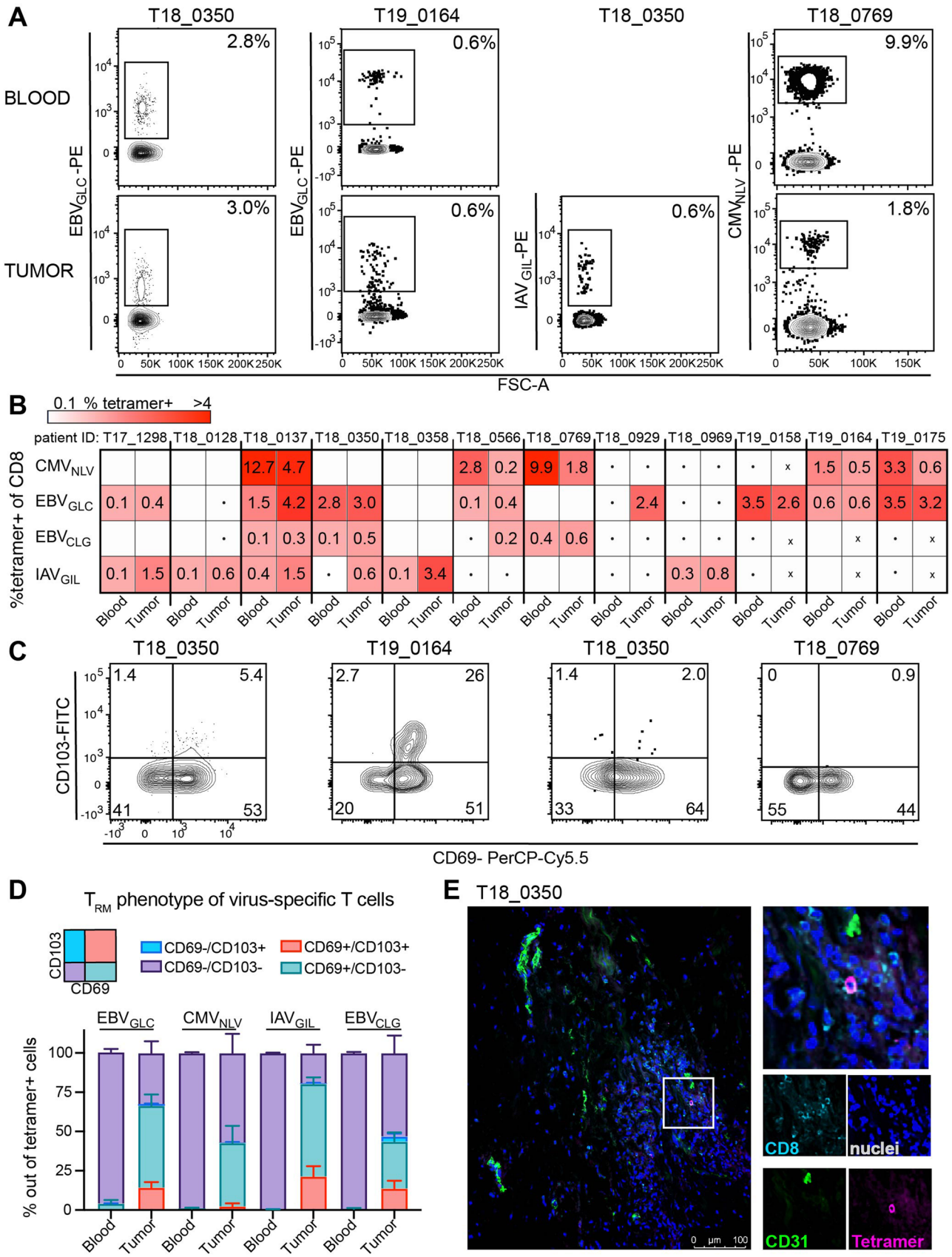
A
T18_0350
T19_0164
T18_0350
T18_0769
BLOOD
TUMOR
2.8%
3.0%
0.6%
0.6%
0.6%
9.9%
1.8%
EBVGLC-PE
IAVGIL-PE
CMVNLV-PE
FSC-A
B
0.1 % tetramer+ >4
patient ID: T17_1298 T18_0128 T18_0137 T18_0350 T18_0358 T18_0566 T18_0769 T18_0929 T18_0969 T19_0158 T19_0164 T19_0175
%tetramer+ of CD8
CMVNLV
EBVGLC
EBVCLG
IAVGIL
Blood Tumor
C
T18_0350
T19_0164
T18_0350
T18_0769
1.4 5.4 41 53
2.7 26 20 51
1.4 2.0 33 64
0 0.9 55 44
CD103-FITC
CD69- PerCP-Cy5.5
D
TRM phenotype of virus-specific T cells
CD103
CD69
CD69-/CD103+
CD69+/CD103+
CD69-/CD103-
CD69+/CD103-
EBVGLC CMVNLV IAVGIL EBVCLG
% out of tetramer+ cells
Blood Tumor
E
T18_0350
0 µm 100
CD8
nuclei
CD31
Tetramer

◂**Fig. 1** Virus-specific memory CD8 + T cells populate GBM and have a T_{RM} phenotype. **a** Patient glioblastoma tumors and paired blood stained for HLA-A*02 + tetramers specific for EBV (EBV_{GLC} and EBV_{CLG}), CMV (CMV_{NLV}), and Influenza A virus (IAV_{GIL}). Gated on CD8 + CD3 + cells. **b** The frequency (%) of tetramer-positive populations out of CD8 + /CD3 + T cells in paired blood and glioblastoma tumors across multiple patients. Dots indicate not enough total CD8 + T cells were acquired to get an accurate measurement; X indicates data was not collected; Blank indicates tetramer + cells were not detected. **c** Phenotype of tetramer + cells gated on in (**a**). **d** Quantification of CD69/CD103 phenotype of tetramer + cells in all patient populations in blood and paired tumors. **e** Representative in situ tetramer immunofluorescence staining of glioblastoma tumor. Magenta, EBV/Flu tetramer; Teal, CD8; Blue, 4',6-diamidino-2-phenylindole (DAPI)-stained nuclei; Green, CD31. White scale bar = 100 µm

and phenotype of virus-specific T cells in mouse and human GBM with the goal of harnessing their functions as a tumor immunotherapy. Memory T cells specific for influenza A virus (IAV), Epstein–Barr virus (EBV), and/or cytomegalovirus (CMV) were present in all clinical glioblastoma samples studied. These T cells expressed phenotypic markers of tissue residency (CD69 and CD103) and were able to respond to viral peptide, triggering immune activation in explanted patient tumors. Virus-specific T cells were also present in the microenvironment of murine glioblastoma models. Reactivation of these T cells via PAT induced immune activation, with associated improved survival. These findings establish virus-specific memory T cells as a part of the glioblastoma tumor immune environment and provide a foundation for harnessing them as a tumor immunotherapy.

Results

Virus-specific CD8 + T cells populate human GBM tumors

To determine the extent to which virus-specific CD8 + T cells occupy human glioblastomas, we constructed HLA-A*02:01-specific tetramers loaded with immunodominant peptides derived from the common viral infections influenza A virus (IAV), cytomegalovirus (CMV), and Epstein–Barr virus (EBV). We stained T cells isolated from patient tumors following standard of care surgical resection. This included 12 individuals ranging from 29 to 68 years of age, and an equal number of males and females (Supplemental Table 1). Memory CD8 + T cells specific for common viral infections consistently populated glioblastoma tumors, and often, T cells specific for a single viral epitope made up over 1% of the total CD8 + T cell population in the tumor (Fig. 1a, 1b). Of note, in all patients where a population of virus-specific T cells was identified in blood (when available), a corresponding population was identified in tumor samples when sufficient tissue was provided for analysis. When stratified by sex, there was no difference in the proportion of patients with detectable tetramer-positive cells, regardless of viral specificity. However, when stratified by age, we observed a higher proportion of patients > 50 years with detectable CMV-specific T cells in the blood and tumor compared to patients < 50, consistent with previous studies in peripheral blood (Supplemental Fig. 1) [16]. We found that most antiviral T cells, regardless of viral specificity, expressed CD69 and a subset also expressed CD103 (Fig. 1c, 1d). CD69 and CD103 are canonical T_{RM} markers and were not expressed by T cells in venous blood, suggesting that these cells were within tumors and not blood contaminants [17]. Using in situ tetramer staining, we visually confirmed that virus-specific T cells were indeed in the tissue, as illustrated by localization outside of CD31 + vascular endothelial cells (Fig. 1e). These data demonstrate the presence of virus-specific CD8 + T cells in human GBM tumors which express markers of tissue residency.

Virus-specific memory T cells perform sensing and alarm functions in human GBM

T_{RM} have been described as having a 'sensing and alarm' function; upon antigen recognition in tissues, they trigger a broad local antimicrobial response [9, 12, 13]. The GBM tumor environment is notoriously immunosuppressive and, given the T_{RM}-phenotype of virus-specific T cells in GBM tumors, we tested if these cells could reactivate and perform sensing and alarm functions to reverse this suppression. We first established ex vivo organotypic slice cultures with five HLA-A2 + GBM tumors. This method preserves the tumor environment while promoting tissue survival through culturing on transwell inserts, allowing for sufficient oxygenation [18]. Each patient was screened for tetramer-positive cells in blood and based on these results, we added relevant viral peptides or vehicle control to autologous slice cultures (Fig. 2a). By adding free peptide comprised only of CD8 + T cell epitopes, we obviated the need for antigen presenting cell processing and were able to attribute any transcriptional changes observed specifically to antiviral CD8 + T cell activation within the tumor. Nine hours following peptide addition, we harvested tumor slices and performed RNAseq on the whole tissue. We found significant differences in gene expression between control and viral peptide treatment in 4 of the 5 tumors (Fig. 2b). Several upregulated genes were the same as previously published in healthy tissue upon T cell reactivation including IFNγ, and the chemokines, CXCL9, CXCL10, and CXCL11 (Fig. 2b) [12, 13]. We performed ingenuity pathway analysis on the gene set with the most differentially expressed genes (T18_0969) and identified

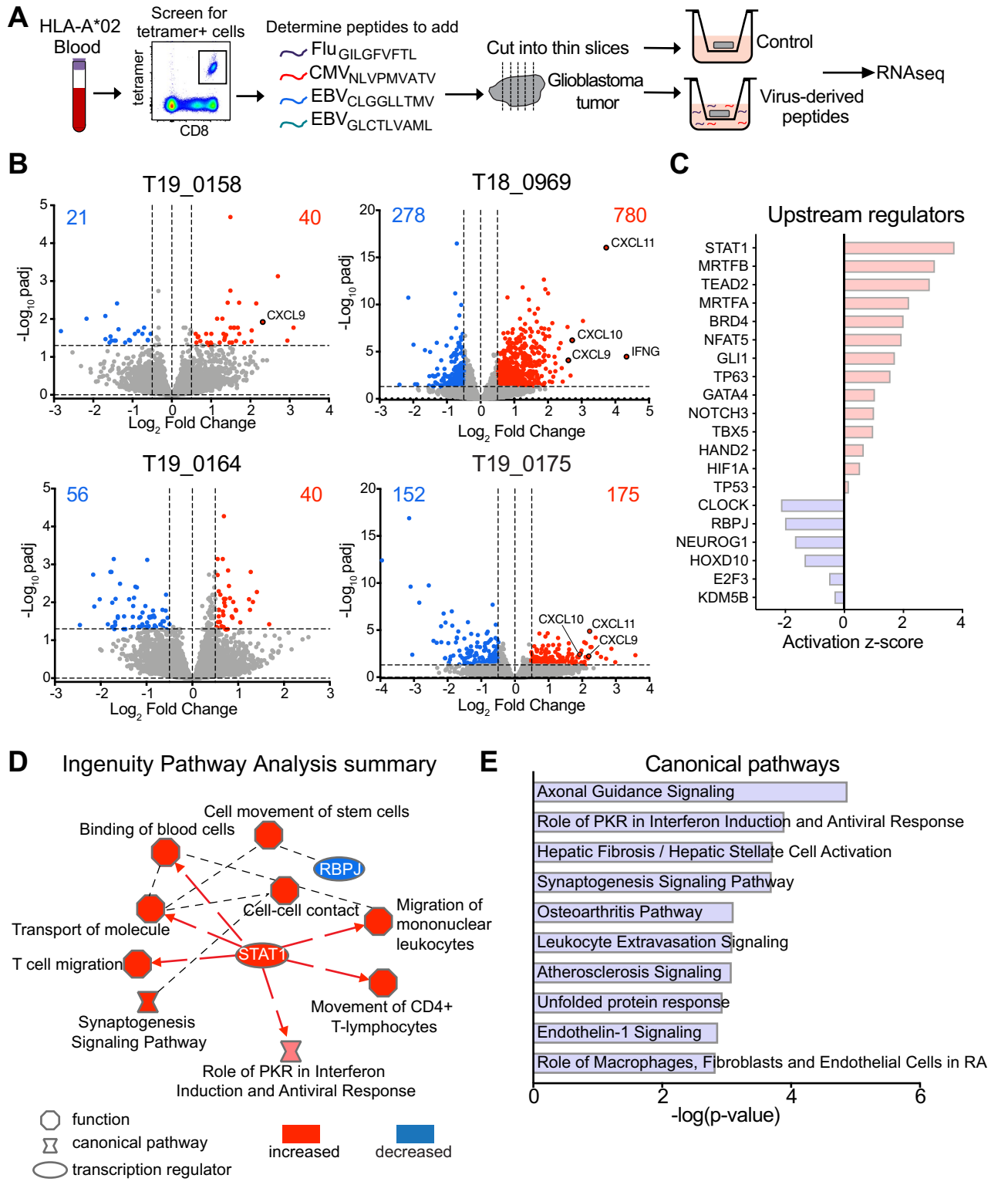

Fig. 2 Virus-specific memory T cells perform sensing and alarm functions in human GBM. **a** Schematic of experimental setup. **b** Volcano plot of four patient tumors showing differentially expressed genes in viral peptide treated tumors versus control. **C–e** Ingenuity pathway analysis results from patient T18_0969; **c** upstream regulators; **d** graphical summary of IPA results: Blue: inhibited node z-score ≤ 2, Red: activated node z-score ≥ 2 **e** Upregulated canonical pathways

STAT1 regulated interferon signaling and antiviral pathways (Fig. 2c). Further analysis revealed an upregulation of functions and pathways important for antiviral responses and lymphocyte migration (Fig. 2d and e). We also observed signatures such as 'Axonal Guidance Signaling' and 'Synaptogenesis Signaling Pathway,' reflective of the tissue of origin. In all, these data indicate that virus-specific memory T cells in human GBM tumors can perform sensing and alarm functions and thus may be a tractable therapeutic target for transforming the suppressive tumor environment.

Establishment of T_{RM}-phenotype cells in mouse GBM following diverse infections

We hypothesized that reactivating memory T cells with viral peptides in vivo could trigger immune activating alarm functions and promote anti-tumor responses. To test this, we first sought to establish a mouse model of GBM which harbors virus-specific memory T cells, mimicking what we observed in humans. Because of the nature of typical preclinical mouse models that are housed in specific pathogen free conditions, thus lacking physiologic infectious experience, there are very few memory T cells established in nonlymphoid tissues [19]. To establish a trackable population of virus-specific memory T cells, we took advantage of transgenic T cells specific for model antigens. We transferred Thy1.1 or CD45.1 naïve transgenic CD8 + T cells specific for the ovalbumin protein (ova), termed OT-I T cells, or the gp33 epitope of lymphocytic choriomeningitis virus (LCMV), termed P14 T cells, into CD45.2 congenically distinct wild type C57BL/6 host mice. One day after T cell transfer, we infected mice with pathogens of interest expressing the antigens ova or gp33; LCMV, Influenza A virus strain PR8 expressing gp33 ($PR8_{gp33}$), or vesicular stomatitis virus (VSV_{ova}) intranasally, or VSV_{ova} intravenously (Fig. 3). These infections result in the durable establishment of broadly distributed memory T cells, including in the brain [20–24]. Greater than 30 days post-infection (referred to as immune memory mice), we then established GBM tumors using an orthotopic model by intracranially implanting syngeneic GBM cell lines. GL261 is a commonly used GBM cell line which harbors a KRAS mutation, p53 mutations, and high expression of c-myc [25]. GL261 cells were implanted intracranially into immune memory mice, and we assessed T cell infiltration by histology at 14–16 days post-GL261 implantation. Irrespective of the virus or route of infection, we found abundant virus-specific OT-I and P14 T cells in GBM tumors (Fig. 3a-d). This observation was also seen in a second tumor model using the 005 cell line, which has HRAS and AKT mutations, and was recently shown to more closely resemble the immune landscape of human glioblastoma (Fig. 3d) [26, 27]. In both the GL261 and 005 models, we observed virus-specific memory T cells expressing CD69 and a subset co-expressed CD69 and CD103 (Fig. 3e, f). This T_{RM} phenotype was most prominent in IAV and VSV intranasal infections, but all infection modalities produced this phenotype, modeling what we observed in human GBM tumors (Fig. 3e, f). In summary, memory CD8 + T cells established by diverse viral infections populate mouse GBM models and can express markers associated with tissue residency.

Virus-specific memory T cells can perform sensing and alarm functions in mouse GBM

We next tested if virus-specific T cells can be reactivated in response to cognate viral peptides in the highly immunosuppressive GBM tumor environment. We focused on the intranasal VSV_{ova} infection model as it generated antiviral memory T cells in tumors that more closely resembled those found in humans. We injected viral (SIINFEKL) or irrelevant control (gp33) peptides intracranially into GL261 or 005 tumors and assessed T_{RM} activation nine hours later (Fig. 4a). Consistent with T_{RM} activation, we found that OT-I T cells upregulated IFNγ and CD25 (IL-2Ra) in both tumor models, although a greater percentage of cells appeared activated in GL261 than in 005 tumors (Fig. 4b, e). We assessed OT-I activation at a later timepoint, 48 h post-peptide injection, and found an upregulation of cytotoxic granzyme B and the proliferation marker, Ki67, in GL261 tumors which was not seen in 005 tumors at this timepoint (Fig. 4c, f). Despite the increase in Ki67, however, we did not observe an increase in the number of virus-specific T_{RM} 48 h later (Fig. 4d, g).

We next assessed if T cell reactivation triggered activation of surrounding immune cells, as previously observed in healthy murine skin and female reproductive tract, and in autochthonous and orthotopic mouse models of melanoma [3, 12, 13]. We observed that in both GL261 and 005 tumor models, as a consequence of antigen recognition by memory CD8 + T cells, NK cells became activated, upregulating granzyme B within 48 h (Fig. 5a). This correlated with a modest increase in Ki67, but paradoxically, a decrease in NK cell numbers in GL261 tumors with no difference in 005 tumors (Fig. 5a). We assessed activation of non-OT-I 'bystander' memory CD8 + T cells and found an increase in granzyme B expression in T cells isolated from GL261 tumors, but not 005, and no changes in Ki67 or total numbers of cells (Fig. 5b). Like NK cells, we observed a small but significant decrease in non-OT-I CD8 + T cell numbers in GL261 tumors (Fig. 5b). These data demonstrate that virus-specific T cells can be reactivated in GBM tumors, and this can lead to immune activation of other cell types, albeit more so in the GL261 model than 005.

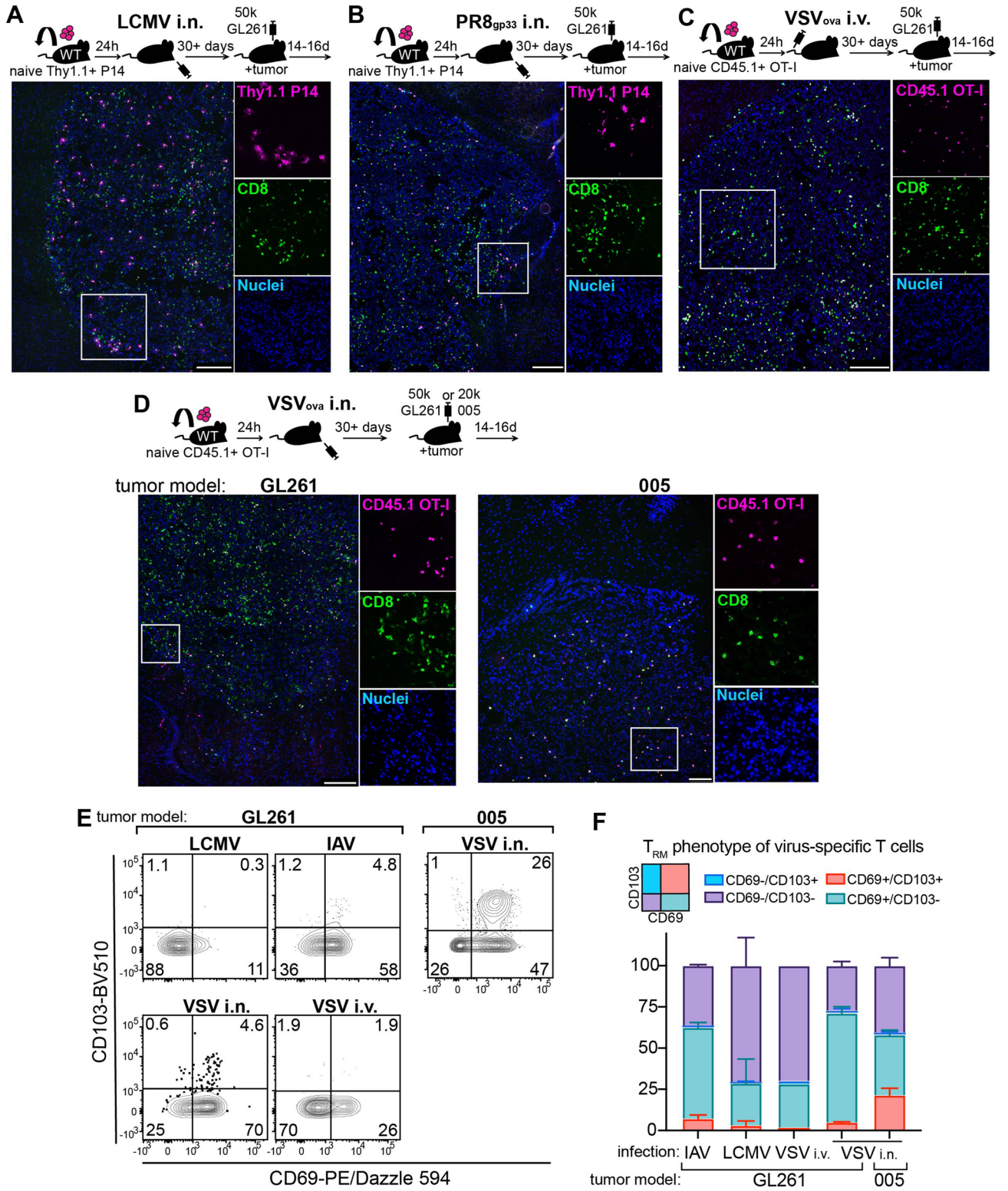

Fig. 3 Establishment of T_{RM} phenotype cells in mouse GBM following diverse infections. **a–d** Schematic of experimental setup utilizing transgenic T cells specific for antigens expressed by concurrent indicated infection, with corresponding immunofluorescence staining of GBM tumor. Magenta, transgenic T cells (P14 or OT-I); Green, CD8; Blue, DAPI stained nuclei. Scale bars = 100 µm. **e** Representative flow plots gated on transgenic T cells within GBM tumors. **f** Quantification of E indicating % of total P14 or OT-I populations expressing CD69/CD103

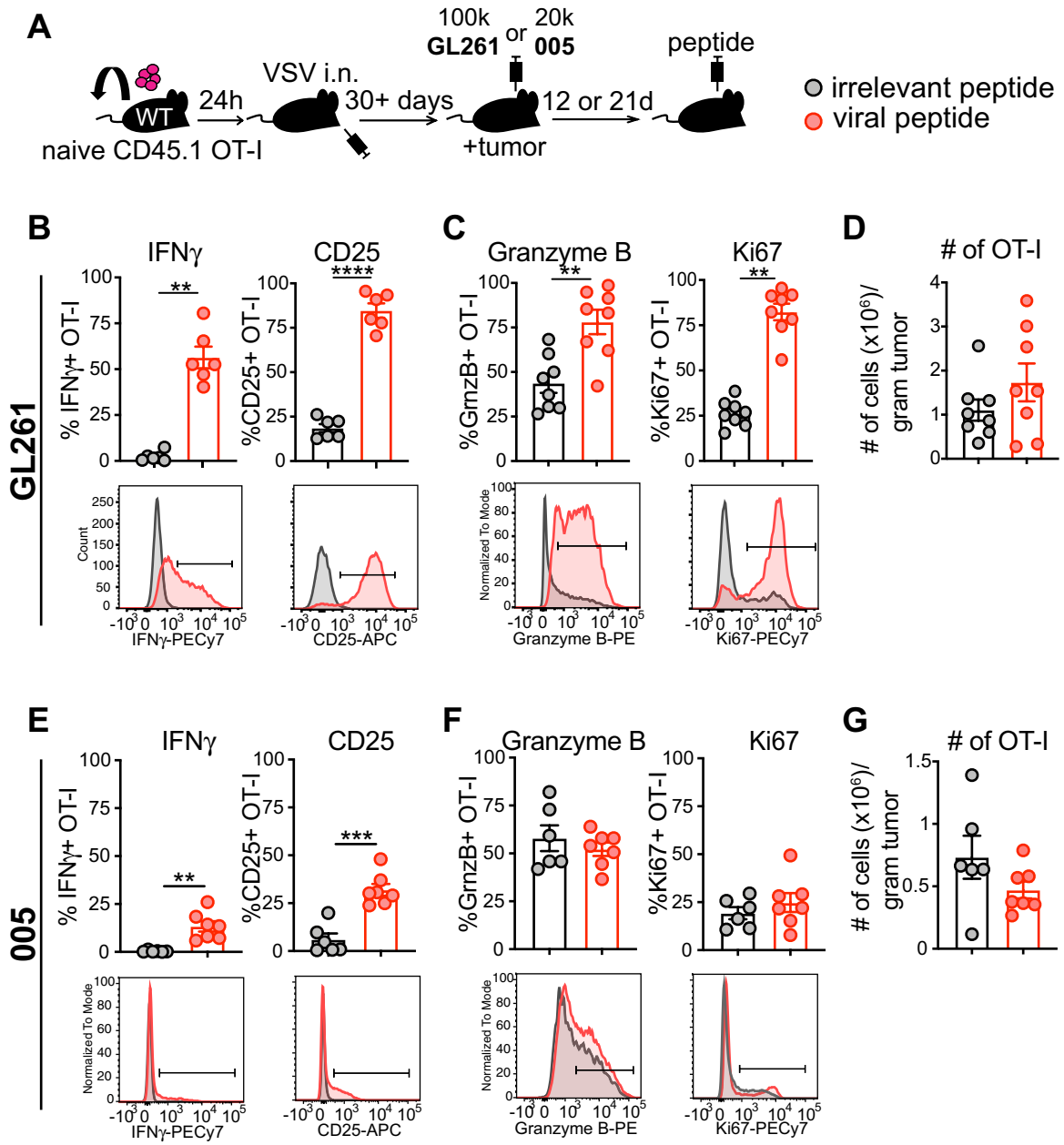

Fig. 4 Virus-specific memory T cells reactivate in mouse GBM. **a** Schematic of experimental setup. **b, e** Proportion of IFNγ+, and CD25+OT-I in GL261 (**b**) or 005 (**e**) tumors 9 h following intratumoral injection of irrelevant (gray) or viral SIINFEKL peptide (red). Representative flow plots below graphs. **c, f** Proportion of OT-I T cells expressing granzyme B and Ki67 48 h post-peptide injection of GL261 (**c**) or 005 (f) tumors, with representative flow plots below. **d** Quantification by flow cytometry of OT-I T cells in GL261 (**d**) or 005 (**g**) tumors 48 h post-challenge with control, or viral SIINFEKL peptide. Statistical significance was determined by unpaired two-tailed *t*-test (**b**, CD25 and **c**) and unpaired two-tailed Mann–Whitney test (**b,** IFNγ) where $^{**}p < 0.01$, $^{***}p < 0.001$, $^{****}p < 0.0001$

Therapeutic efficacy of peptide alarm therapy

Given the observed immune activation following peptide alarm therapy, we hypothesized that antiviral memory T cell reactivation could be leveraged as a GBM therapy to counteract the suppressive tumor environment and promote an anti-tumor response. To test this, we intracranially inoculated OT-I immune memory mice with GL261 or 005 tumors. We then performed peptide alarm therapy by intratumorally injecting viral-derived SIINFEKL peptide or irrelevant control peptide twice, 48 h apart. We then assessed survival following therapy. We saw a significant increase in survival following treatment of mice with 005 tumors, but not GL261 (Fig. 6). While all mice still succumbed to

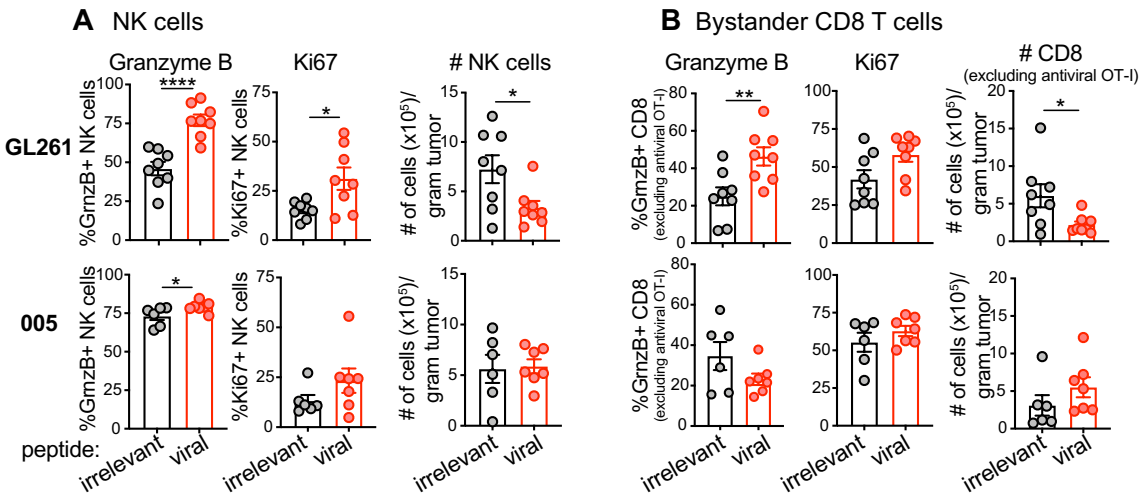

Fig. 5 Virus-specific memory T cells can perform sensing and alarm functions in mouse GBM. Mice with T cell memory and GBM tumors were established as in Fig. 4. **a** Proportion of NK cells expressing granzyme B and Ki67, and quantification of NK cells by flow cytometry in GL261 (top) or 005 (bottom) tumors 48 h post-challenge with control or viral SIINFEKL peptide. **b** Proportion of non-OT-I memory CD8 + T cells (gated on CD44 +) expressing granzyme B and Ki67, and quantification of cells by flow cytometry in GL261 (top) or 005 (bottom) tumors 48 h post-peptide challenge. Statistical significance was determined by unpaired two-tailed *t*-test (**a** and **b,** granzyme B) and unpaired two-tailed Mann–Whitney test (**b,** # CD8) where *p < 0.05, **p < 0.01, ****p < 0.0001

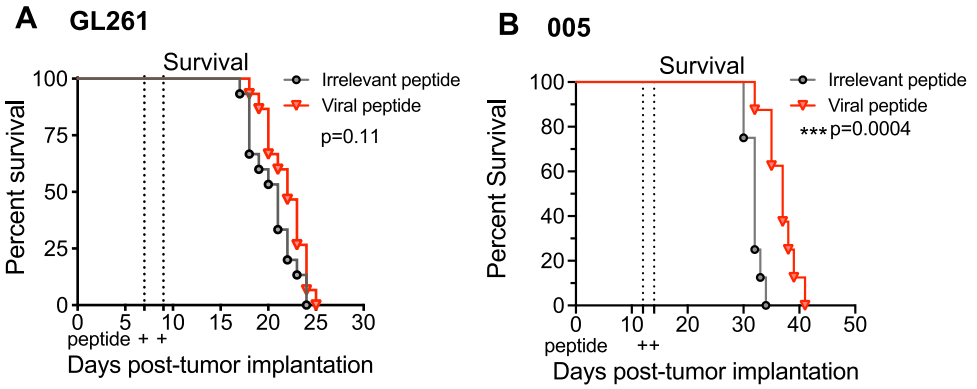

Fig. 6 Therapeutic efficacy of peptide alarm therapy. Mice with T cell memory and GBM tumors were established as in Fig. 4. Survival of mice with GL261 **(a)** or 005 **(b)** GBM tumors receiving two intratumoral injections of irrelevant (black) or viral SIINFEKL (red) peptides twice, 2 days apart. Statistical significance was determined by log-rank Mantel–Cox test where ***p < 0.001. **a** n = 15 mice pooled from three independent experiments. **b** n = 8 mice, pooled from two independent experiments

tumor, the median survival of mice bearing 005 tumors was extended by 5 days (32 to 37 days). These data contrast with the observed increase in immune activation in GL261 than in 005 tumors (Figs. 4 and 5), indicating that, at least at the timepoints examined, the magnitude of CD8 + T or NK cell activation or accumulation in tumors is not necessarily predictive of therapeutic efficacy with PAT in GBM models. In all, these data show that peptide alarm therapy is effective at increasing survival of mice with GBM, but this may depend on the tumor model.

Discussion

This study demonstrates an abundance of virus-specific memory T cells in both mouse and human glioblastoma tumors, establishing these cells as a previously unappreciated but significant part of the GBM tumor immune environment. We further showed that these cells are functional in both human and mouse glioblastomas and that activating antiviral memory T cells is a potential therapeutic approach. Consistently, a majority of these virus-specific memory T cells expressed CD69 and CD103, suggesting

they may be resident within the tumor. The tumor environment is unlike that of healthy tissue, however, and may harbor soluble mediators that promote a T_{RM}-like phenotype, such as TGFβ, which can upregulate CD103 [28], and interferons, which can induce CD69 expression [29]. Future studies will focus on understanding the source and migratory nature of these cells within tumors.

Peptide alarm therapy (PAT) taps into the immune activating functions of T_{RM} by mimicking a local reinfection through delivery of viral-derived peptides in situ. Other groups have employed this strategy as a systemic therapy by conjugating viral-derived peptides to tumor-targeting antibodies, which has demonstrated efficacy against patient derived breast, liver and lung xenograft mouse tumor models [30, 31]. While this may be an attractive delivery approach in some cancers, systemic therapies are often restricted by the blood brain barrier and fail to effectively reach GBM. In a clinical setting, surgery is the standard of care for GBM patients, and it will be important to understand the translatability of PAT delivered to the resected tumor site at the time of surgery. Indeed, it has been shown that CD8 + T cell responses change following surgical resection of glioblastoma tumors in mouse models [27].

While the role of CMV in GBM is controversial, several studies have found CMV antigens in human glioblastoma tumors [32]. These findings have sparked clinical trials using dendritic cell vaccines to promote anti-CMV T cell responses [33], and CMV-specific T cell adoptive therapies [34, 35]. It is worth noting that we found no clear enrichment of CMV-specific T cells in GBM tumors, and moreover, identified EBV and IAV-specific T cells, suggesting broad localization of virus-specific T cells to GBM tumors.

It is interesting that despite an abundance of highly responsive antiviral T cells, we did not observe therapeutic efficacy in the GL261 model but did in 005 (Fig. 6). Our GL261 results contrast with other tumor models we have tested, including a subcutaneous MC38 colon carcinoma, intradermal B16 melanoma, and an autochthonous dermal melanoma model [3]. This suggests that the magnitude of T cell activation is not predicative of therapeutic efficacy and that there may be glioblastoma or central nervous system (CNS) microenvironment influences that mitigate the downstream consequences of T_{RM} reactivation. A deeper understanding of these mechanisms will lend insights into poorly understood T_{RM} biology in the CNS as well as glioblastoma immuno-biology.

In healthy tissue and other murine tumor models, T_{RM} reactivation results in a significant increase in the number of virus-specific T cells, bystander CD8 + T cell and NK cells [3, 12, 36]. Interestingly, this is also supported in humans by a recent study in hepatocellular carcinoma, which demonstrated a link between activated HBV-specific $T_{RM,}$ and infiltration of bystander CD8 + T cells into the tumor [37]. In contrast to these studies, we did not find an increase in T cells or NK cells in GBM tumors following virus-specific T cell activation, and even saw a *decrease* in some of these cell populations. It should be noted that while CD8 + T cells in the tissue versus vasculature were differentially labeled, our analysis represents total NK cells in both compartments. Overall, this indicates that in GBM, canonical T_{RM} functions may not operate as they do in other tissues, and it may be that the restrictions imposed by the blood–brain barrier on immune cell recruitment are not overcome in these mouse models. Understanding how immune cell homing to tumors following PAT occurs in other models (like melanoma) but not in brain tumors will be important for moving this therapy forward and will have implications for our fundamental understanding of T cell surveillance of the brain. It is also likely that systemic immune suppression caused by brain tumors, or interestingly, even the physical injection of peptides, may be restricting therapeutic efficacy [38, 39]. Indeed, it was recently shown that intracranial PBS injection can induce immune suppression, including thymic involution [39]. It will thus be important to explore alternative routes of therapeutic delivery such as intranasal or intravenous.

While the observed therapeutic efficacy was modest, this provides a foundation from which to further optimize PAT and investigate synergizing combination therapies. For example, immune checkpoint inhibitors have poor demonstrated efficacy in GBM clinical trials [40], but we have previously shown that PAT sensitizes normally resistant murine B16 melanoma tumors resulting in tumor clearance [3]. Oncolytic viruses (OV) also present an opportunity for possible therapeutic synergy; there are several active clinical trials testing OVs in glioblastoma, and many of these therapeutics are engineered from viruses to which the population has preexisting immunity, such as herpes simplex virus (HSV), poliovirus, and measles virus [41]. This presents an intriguing possibility that these therapies are reactivating preexisting OV-specific T cells that were generated during prior infections. This also poses an opportunity to engineer OVs to express immunodominant epitopes from common viral infections to reactivate additional preexisting memory T cells in tumors.

In summary, T_{RM}-phenotype cells specific for common viral infections can reactivate in response to in situ delivered viral-derived peptides in murine glioblastoma models and human glioblastoma explants. This reactivation occurred despite the immunosuppressive environment and was able to trigger NK cell immune activation and ultimately prolong survival of mice harboring 005 GBM tumors. This study supports the potential for leveraging virus-specific T_{RM} for GBM therapy.

Materials and methods

Mice

C57BL/6 J (B6) female mice were purchased from The Jackson Laboratory (Bar Harbor, ME) and were maintained in specific-pathogen-free conditions at the University of Minnesota or Dartmouth College. CD90.1$^+$ OT-I, CD45.1$^+$ OT-I, and Thy1.1 + P14 mice were fully backcrossed to C57BL/6 J mice and maintained in our animal colony. Sample size was chosen on the basis of previous experience. No sample exclusion criteria were applied. No method of randomization was used during group allocation, and investigators were not blinded. All mice used in experiments were 5–14 weeks of age. All mice were used in accordance with the Institutional Animal Care and Use Committees guidelines at the University of Minnesota and Dartmouth College.

Adoptive transfers and infections

Immune memory mice were generated by transferring 5×10^4 CD90.1 or CD45.1 OT-I or CD90.1 P14 CD8$^+$ T cells from female mice into naive 6–8-week-old C57BL/6J female mice. One day following transfer, mice were infected with 1×10^6 PFU of vesicular stomatitis virus expressing chicken ovalbumin (VSV_{ova}) i.v., 5×10^4 VSV_{ova} intranasally, 5×10^5 PFU LCMV Armstrong intranasally, or 500 PFU of Influenza A strain PR8 expressing the gp33 epitope of LCMV ($PR8_{gp33}$) intranasally.

Lymphocyte isolation and phenotyping of mouse cells

We used an intravascular staining method to discriminate cells present in the vasculature from cells in the tissue parenchyma, as described, for 12 h timepoints [42]. In brief, we injected mice i.v. with biotin/fluorochrome-conjugated anti-CD8α i.v. Three minutes after the injection, we euthanized the animals and harvested tissues as described [12, 43]. In brief, GBM tumors were removed, digested in Collagenase IV (Sigma) with DNAse for 30 min, then dissociated via gentleMACS Dissociator (Miltenyi Biotec) and lymphocytes purified on a 44/67% Percoll (GE Healthcare) gradient. Isolated mouse cells were stained with antibodies to CD103 (clone 2E7, eBioscience, 17–1031-80), NK1.1 (clone PK136, BioLegend, 108728), CD8a (clone 53–6.7, BioLegend, 100743), IFNγ (clone XMG1.2, BD Biosciences, 54411), CD25 (clone PC61, BD Biosciences, 557192), CD44 (clone IM7, BioLegend, 103059), granzyme B (clone GB11, Invitrogen, GRB04), CD69 (clone H1.2F3, BD Biosciences, 562455), and Ki67 (clone SolA15, Invitrogen, 25-5698-82). All cells were stained at antibody dilutions of 1:100 except for granzyme B (1:30). Cells stained intracellularly (for IFNγ, granzyme B, and Ki67) were permeabilized using Tonbo or ebioscience Fixation/permeabilization kits. Cell viability was determined with Ghost Dye 780 (Tonbo Biosciences). Enumeration of cells was done using PKH26 reference microbeads (Sigma). The stained samples were acquired with LSRII or LSR Fortessa flow cytometers (BD) and analyzed with FlowJo software (Treestar).

Immunofluorescence microscopy

GL261 or 005 tumors were harvested, then fixed in 2% paraformaldehyde for 2 h before being treated with 30% sucrose overnight for cryoprotection. The sucrose-treated tissue was embedded in OCT tissue-freezing medium and frozen in an isopentane liquid bath. Frozen blocks were processed, stained, and imaged including staining with antibodies to CD8-β (YTS156.7.7; BD Biosciences), CD90.1 (OX-7; BD Biosciences), and CD45.1 (A20; Biolegend). Sections were counterstained with 4′,6-diamidino-2-phenylindole dihydrochloride (DAPI) to detect nuclei.

In situ tetramer staining

Human GBM tumors were sliced into thin sections manually with a sharp surgical blade. Sections were incubated overnight at 4 degrees C with 2 µg/mL PE-conjugated HLA-A2 tetramer in PBS supplemented with 2% FBS and DNAse. Sections were then fixed in 2% paraformaldehyde for 2 h before being treated with 30% sucrose overnight for cryoprotection. Tissues were then frozen and sectioned as described above. PE-tetramer was amplified with a polyclonal rabbit-anti-PE antibody at a 1:600 dilution (Novus Biologicals, NB120-7011) followed by goat anti-rabbit Cy3 at a 1:800 dilution (Jackson ImmunoResearch, 111-165-003). Sections were also co-stained with antibodies to human CD8α (clone RPA-T8, eBiosciences) and CD31 (clone WM59, Biolegend) and counterstained with DAPI to detect nuclei.

Tumor models and treatment

50,000 (Fig. 3) or 100,000 (Figs. 4, 5, 6) GL261, or 20,000 005 cells were injected intracranially into mice. Briefly, a burr hole, 1–1.5 mm in diameter was made using a hand drill without damaging the underlying dura mater. Cells were then injected using a Hamilton syringe guided by a stereotaxic frame into the cerebral hemisphere (3 mm deep, 1.8 mm to the right of bregma). Once the target was reached, 3ul of cells was slowly injected into the brain over a 5 min period followed by 5 min rest, after which the syringe was slowly removed to avoid backflow and the burr hole filled with bone wax. For survival studies, mice were monitored

for clinical symptoms, and mice were euthanized when becoming moribund, and the presence of tumor was confirmed postmortem. GL261 cells were maintained in DMEM (Life Technologies) supplemented with 10% Fetal Bovine Serum and penicillin/streptomycin (Cellgro), and 005 cells in DMEM/F12 medium (Life Technologies) with L-glutamine (2 mM; Corning), 1% N2 supplement (ThermoFisher Gibco), heparin (2 µg/mL; Sigma), penicillin/streptomycin (Cellgro), recombinant EGF (20 ng/mL; R&D Systems), and recombinant FGF2 (20 ng/mL;Peprotech).

For local tumor T cell reactivation experiments involving peptides, 0.5 µg of the indicated peptides (New England Peptides) were delivered by direct intratumor injection (as described above) in a volume of 3 µl phosphate buffered saline. Peptides used in mouse studies: KAVYNFATM (gp33) from LCMV (used as control/irrelevant) and SIINFEKL from ovalbumin.

Procurement and processing of human blood and tissue samples

All tumor tissue and blood were obtained from male or female patients age 16–80 undergoing routine surgical resection of solid tumors or tumor metastases. Tumor tissue not required for pathological diagnostic procedures was obtained after surgical resection at the University of Minnesota and collected and de-identified by the Tissue Procurement Facility (BioNet, University of Minnesota). Informed consent was obtained from all subjects. The University of Minnesota Institutional Review Board approved all protocols used. Blood was collected in EDTA collection tubes and tumors were collected in RPMI media containing 5% FBS. All samples were stored at 4 degrees until processed (within 24 h). Specimens reported on were obtained from HLA*A02 + patients that had sufficient tetramer + cells for analysis by flow cytometry. Human blood was processed by Ficoll gradient. Tumors were minced and digested in Collagenase type IV with DNAse for 30 min then dissociated via gentleMACS Dissociator, and lymphocytes purified on a 44/67% Percoll (GE Healthcare) gradient. Lymphocytes were stained for antihuman HLA-A2 (clone BB7.2, BioLegend, 343324), CCR7 (clone G043H7, BioLegend, 353208), CD45RO (clone UCHL1, BioLegend, 304232), CD8α (clone SK1, BD Biosciences, 561945), CD3e (clone SP34-2, BD Biosciences, 557917), CD4 (clone L200, BD Biosciences, 551980), CD69 (clone FN50, BioLegend, 310926), and CD103 (clone HML-1, Beckman Coulter, IM1856U). Cells were stained at antibody dilutions of 1:30. Samples were also stained for PE conjugated HLA-A*02 tetramers (made in house) for EBV_{GLC}, EBV_{CGL}, CMV_{NLV}, and IAV_{GIL}. Viability was assessed by live/dead staining with GhostDye510 (Tonbo biosciences).

Transwell cultures and RNA isolation

Tumors were sliced into thin sections manually with a sharp surgical blade. Sections were then incubated in RPMI media containing 10% FBS, L-glutamine, sodium pyruvate, penicillin/streptomycin, HEPES, nonessential amino acids, and beta-mercaptoethanol on 24-well polycarbonate Transwell inserts with a 0.4 µm pore size (Corning) and maintained in 5% CO_2 and atmospheric oxygen levels [18]. Tissues were incubated with viral peptides at 10 µg/mL or in equal volume of DMSO for 9 h. Tissues with poor viability after culture were excluded. Tumor sections were stored in RNAlater (ThermoFisher) at 4 degrees overnight, then stored at -80 until further processing. For RNA isolation, tissue was thawed on ice in 1 mL TRIZOL (Invitrogen), then homogenized with a Tissue Tearor homogenizer, BioSpec. RNA was then isolated following the TRIZOL recommended protocol. Resulting RNA was then further purified using Qiagen RNA Cleanup Kit. Peptides used in human studies: CLGGLLTMV (EBV_{CLG}), GLCTLVAML (EBV_{GLC}), NLVPMVATV (CMV_{NLV}), GILGFVFTL (IAV_{GIL}).

RNA library preparation and sequencing

mRNA libraries were generated using the TruSeq Stranded mRNA Library Prep kit (Illumina) and sequenced on an Illumina HiSeq 2500 in 50-base paired-end reactions. Fastq files were verified for quality control using the fastqc software package. Low-quality segments and adapters were trimmed using Trimmomatic. Quality-filtered reads were aligned to the human genome GRCh38 using Hisat [44]. Differentially expressed genes were determined using the DESeq2 R package [45] where false-discovery rate (FDR) < 0.05 was considered significant. Upstream transcriptional regulators, canonical pathways, and summary plots were generated through the use of ingenuity pathway analysis (IPA, QIAGEN Inc., https://www.qiagenbioinformatics.com/products/ingenuity-pathway-analysis) [46].

Statistics

Data were subjected to the Shapiro–Wilk normality test to determine whether they were sampled from a Gaussian distribution. If a Gaussian model of sampling was satisfied, parametric tests (unpaired two-tailed Student's *t*-test for two groups and one-way ANOVA with Bonferroni multiple comparison test for more than two groups) were used. If the samples deviated from a Gaussian distribution, nonparametric tests were used (Mann–Whitney U test for two groups, Kruskal–Wallis with Dunn's multiple comparison test for more than two groups). Survival data were analyzed by Kaplan–Meier survival curves, and comparisons determined by log-rank (Mantel–Cox) test. All statistical analysis was

done in GraphPad Prism (GraphPad Software Inc.). $P < 0.05$ was considered significant.

Cell definitions

Memory CD8 + T cell: CD8 + T cells that have encountered antigen (when known) more than 30 days ago and/or are CD44-positive (mouse), or CCR7/CD45RA-negative (human).

Supplementary Information The online version contains supplementary material available at https://doi.org/10.1007/s00262-021-03125-w.

Acknowledgements The authors thank Dr. Ryan Langlois for PR8-gp33, the NIH Tetramer Facility for HLA-A*02:01 heavy chain plasmid, the Minnesota Supercomputing Institute for assistance with RNA sequencing, and University of Minnesota (UMN) BioNet for assistance with human samples.

Funding This work was supported by a UMN SPORE Program Project Planning grant (DM, CCC), NCI 1R01CA238439 (DM), Humor to Fight the Tumor Foundation (JN), and support from the Norris Cotton Cancer Center, NCI 5P30CA023108-42 (PR). The authors have no relevant financial or non-financial interests to disclose. The datasets generated during and/or analyzed during the current study are available from the corresponding author on request.

Data Accessability RNAseq data are deposited to the GEO database under the accession code GSE185029.

References

1. Yu MW, Quail DF (2021) Immunotherapy for glioblastoma: current progress and challenge. Front Immunol 12:676301. https://doi.org/10.3389/fimmu.2021.676301
2. Lim M, Xia Y, Bettegowda C, Weller M (2018) Current state of immunotherapy for glioblastoma. Nat Rev Clin Oncol 15:422–442
3. Rosato PC, Wijeyesinghe S, Stolley JM et al (2019) Virus-specific memory T cells populate tumors and can be repurposed for tumor immunotherapy. Nat Commun 10:567. https://doi.org/10.1038/s41467-019-08534-1
4. Scheper W, Kelderman S, Fanchi LF et al (2018) Low and variable tumor reactivity of the intratumoral TCR repertoire in human cancers. Nat Med 359:1350–1394
5. Chiou S-H, Tseng D, Reuben A et al (2021) Global analysis of shared T cell specificities in human non-small cell lung cancer enables HLA inference and antigen discovery. Immunity 54:586-602.e8. https://doi.org/10.1016/j.immuni.2021.02.014
6. Duhen T, Duhen R, Montler R et al (2018) Co-expression of CD39 and CD103 identifies tumor-reactive CD8 T cells in human solid tumors. Nat Commun 9:56
7. Andersen RS, Thrue CA, Junker N et al (2012) Dissection of T-cell antigen specificity in human melanoma. Cancer Res 72:1642–1650. https://doi.org/10.1158/0008-5472.CAN-11-2614
8. Simoni Y, Becht E, Fehlings M et al (2018) Bystander CD8 + T cells are abundant and phenotypically distinct in human tumour infiltrates. Nature 557:575
9. Schenkel JM, Fraser KA, Vezys V, Masopust D (2013) Sensing and alarm function of resident memory $CD8^+$ T cells. Nat Immunol 14:509–513. https://doi.org/10.1038/ni.2568
10. Rosato PC, Beura LK, Masopust D (2017) Tissue resident memory T cells and viral immunity. Curr Opin Virol 22:44–50
11. Rosato PC, Wijeyesinghe S, Stolley JM, Masopust D (2020) Integrating resident memory into T cell differentiation models. Curr Opin Immunol 63:35–42. https://doi.org/10.1016/j.coi.2020.01.001
12. Schenkel JM, Fraser KA, Beura LK et al (2014) Resident memory CD8 T cells trigger protective innate and adaptive immune responses. Science 346:98–101. https://doi.org/10.1126/science.1254536
13. Ariotti S, Hogenbirk MA, Dijkgraaf FE et al (2014) T cell memory. Skin-resident memory $CD8^+$ T cells trigger a state of tissue-wide pathogen alert. Science 346:101–105. https://doi.org/10.1126/science.1254803
14. Dhodapkar MV, Dhodapkar KM (2020) Tissue-resident memory-like T cells in tumor immunity: clinical implications. Semin Immunol 49:101415. https://doi.org/10.1016/j.smim.2020.101415
15. Vasquez JC, Huttner A, Zhang L et al (2017) SOX2 immunity and tissue resident memory in children and young adults with glioma. J Neurooncol 134:41–53. https://doi.org/10.1007/s11060-017-2515-8
16. Khan N, Shariff N, Cobbold M et al (2002) Cytomegalovirus seropositivity drives the CD8 T cell repertoire toward greater clonality in healthy elderly individuals. J Immunol 169:1984–1992. https://doi.org/10.4049/jimmunol.169.4.1984
17. Szabo PA, Miron M, Farber DL (2019) Location, location, location: tissue resident memory T cells in mice and humans. Sci Immunol 4:eaas9673. https://doi.org/10.1126/sciimmunol.aas9673
18. Davies EJ, Dong M, Gutekunst M et al (2015) Capturing complex tumour biology *in vitro*: histological and molecular characterisation of precision cut slices. Sci Rep 5:17187
19. Beura LK, Hamilton SE, Bi K et al (2016) Normalizing the environment recapitulates adult human immune traits in laboratory mice. Nature 532:512–516
20. Wakim LM, Woodward-Davis A, Liu R et al (2012) The molecular signature of tissue resident memory CD8 T cells isolated from the brain. J Immunol 189:1201305–1203471
21. Wijeyesinghe S, Beura LK, Pierson MJ et al (2021) Expansible residence decentralizes immune homeostasis. Nature. https://doi.org/10.1038/s41586-021-03351-3
22. Hawke S, Stevenson PG, Freeman S, Bangham CR (1998) Long-term persistence of activated cytotoxic T lymphocytes after viral infection of the central nervous system. J Exp Med 187:1575–1582
23. Urban SL, Jensen IJ, Shan Q et al (2020) Peripherally induced brain tissue–resident memory CD8 + T cells mediate protection against CNS infection. Nat Immunol 21:938–949. https://doi.org/10.1038/s41590-020-0711-8
24. Nelson CE, Thompson EA, Quarnstrom CF et al (2019) Robust iterative stimulation with self-antigens overcomes CD8+ T cell tolerance to self- and tumor antigens. Cell Rep 28:3092-3104.e5. https://doi.org/10.1016/j.celrep.2019.08.038
25. Szatmári T, Lumniczky K, Désaknai S et al (2006) Detailed characterization of the mouse glioma 261 tumor model for experimental glioblastoma therapy. Cancer Sci 97:546–553
26. Marumoto T, Tashiro A, Friedmann-Morvinski D et al (2009) Development of a novel mouse glioma model using lentiviral vectors. Nat Med 15:110–116. https://doi.org/10.1038/nm.1863
27. Khalsa JK, Cheng N, Keegan J et al (2020) Immune phenotyping of diverse syngeneic murine brain tumors identifies immunologically distinct types. Nat Commun 11:3912. https://doi.org/10.1038/s41467-020-17704-5
28. Casey KA, Fraser KA, Schenkel JM, et al (2012) Antigen-independent differentiation and maintenance of effector-like resident

memory T cells in tissues. J Immunol (Baltimore, Md: 1950) 188:4866–4875
29. Shiow LR, Rosen DB, Brdicková N et al (2006) CD69 acts downstream of interferon-alpha/beta to inhibit S1P1 and lymphocyte egress from lymphoid organs. Nature 440:540–544. https://doi.org/10.1038/nature04606
30. Millar DG, Ramjiawan RR, Kawaguchi K et al (2020) Antibody-mediated delivery of viral epitopes to tumors harnesses CMV-specific T cells for cancer therapy. Nat Biotechnol 38:420–425. https://doi.org/10.1038/s41587-019-0404-8
31. Sefrin JP, Hillringhaus L, Mundigl O et al (2019) Sensitization of tumors for attack by virus-specific CD8+ T-cells through antibody-mediated delivery of immunogenic T-cell epitopes. Front Immunol 10:1962. https://doi.org/10.3389/fimmu.2019.01962
32. Rahman M, Dastmalchi F, Karachi A, Mitchell D (2018) The role of CMV in glioblastoma and implications for immunotherapeutic strategies. Oncoimmunology 8:e1514921. https://doi.org/10.1080/2162402X.2018.1514921
33. Batich KA, Mitchell DA, Healy P et al (2020) Once, twice, three times a finding: reproducibility of dendritic cell vaccine trials targeting cytomegalovirus in glioblastoma. Clin Cancer Res 26:5297–5303. https://doi.org/10.1158/1078-0432.CCR-20-1082
34. Smith C, Lineburg KE, Martins JP et al (2020) Autologous CMV-specific T cells are a safe adjuvant immunotherapy for primary glioblastoma multiforme. J Clin Invest 130:6041–6053. https://doi.org/10.1172/JCI138649
35. Weathers S-P, Penas-Prado M, Pei B-L et al (2020) Glioblastoma-mediated immune dysfunction limits CMV-specific T cells and therapeutic responses: results from a phase I/II trial. Clin Cancer Res 26:3565–3577. https://doi.org/10.1158/1078-0432.CCR-20-0176
36. Beura LK, Mitchell JS, Thompson EA et al (2018) Intravital mucosal imaging of CD8+resident memory T cells shows tissue-autonomous recall responses that amplify secondary memory. Nat Immunol 19:173–182
37. Cheng Y, Gunasegaran B, Singh HD et al (2021) Non-terminally exhausted tumor-resident memory HBV-specific T cell responses correlate with relapse-free survival in hepatocellular carcinoma. Immunity 54:1825-1840.e7. https://doi.org/10.1016/j.immuni.2021.06.013
38. Chongsathidkiet P, Jackson C, Koyama S et al (2018) Sequestration of T cells in bone marrow in the setting of glioblastoma and other intracranial tumors. Nat Med 24:1459–1468. https://doi.org/10.1038/s41591-018-0135-2
39. Ayasoufi K, Pfaller CK, Evgin L et al (2020) Brain cancer induces systemic immunosuppression through release of non-steroid soluble mediators. Brain 143:3629–3652. https://doi.org/10.1093/brain/awaa343
40. Akintola OO, Reardon DA (2021) The current landscape of immune checkpoint blockade in glioblastoma. Neurosurg Clin N Am 32:235–248. https://doi.org/10.1016/j.nec.2020.12.003
41. Liu P, Wang Y, Wang Y et al (2020) Effects of oncolytic viruses and viral vectors on immunity in glioblastoma. Gene Ther. https://doi.org/10.1038/s41434-020-00207-9
42. Anderson KG, Mayer-Barber K, Sung H et al (2014) Intravascular staining for discrimination of vascular and tissue leukocytes. Nat Protoc 9:209–222. https://doi.org/10.1038/nprot.2014.005
43. Steinert EM, Schenkel JM, Fraser KA et al (2015) Quantifying memory CD8 T cells reveals regionalization of immunosurveillance. Cell 161:737–749. https://doi.org/10.1016/j.cell.2015.03.031
44. Kim D, Langmead B, Salzberg SL (2015) HISAT: a fast spliced aligner with low memory requirements. Nat Methods 12:357–360
45. Love MI, Huber W, Anders S (2014) Moderated estimation of fold change and dispersion for RNA-seq data with DESeq2. Genome Biol 15:550
46. Krämer A, Green J, Pollard J, Tugendreich S (2014) Causal analysis approaches in ingenuity pathway analysis. Bioinformatics 30:523–530. https://doi.org/10.1093/bioinformatics/btt703